

1 **Increasing Multiyear Sea Ice Loss in the Beaufort Sea: A New Export Pathway**
2 **for the Diminishing Multiyear Ice Cover of the Arctic Ocean**
3

4 David G. Babb¹ (david.babb@umanitoba.ca) (ORCID: 0000-0002-7427-8094)

5 Ryan J. Galley^{2,3} (ORCID: 0000-0002-5403-9694)

6 Stephen E.L. Howell⁴ (ORCID: 0000-0002-4848-9867)

7 Jack C. Landy⁵ (ORCID: 0000-0002-7372-1007)

8 Julienne C. Stroeve^{1,6,7} (ORCID: 0000-0001-7316-8320)

9 David G. Barber¹ (ORCID: 0000-0001-9466-329)

10
11 ¹ Centre for Earth Observation Science, University of Manitoba, Winnipeg, MB,
12 Canada

13 ² Department of Environment and Geography, University of Manitoba, Winnipeg,
14 MB, Canada

15 ³ Department of Fisheries and Oceans Canada, Winnipeg, MB, Canada.

16 ⁴ Environment and Climate Change Canada, Toronto, ON, Canada

17 ⁵ Department of Physics and Technology, UiT The Arctic University of Norway, 9037
18 Tromsø, Norway;

19 ⁶ CPOM, London, United Kingdom

20 ⁷ NSIDC, Boulder, Colorado, United States
21

22
23 **Keywords:**

24 Sea ice; Multiyear ice; Beaufort Sea; Arctic Ocean; Sea ice dynamics; Beaufort Gyre
25

26 **Key Points:**

- 27 1. MYI area loss in the Beaufort Sea quadrupled from 46,000 km² yr⁻¹ in 1997-
28 2001 to 183,000 km² yr⁻¹ in 2017-2021.
29 2. MYI area loss peaked at 385,000 km² in 2018, which is close to the annual
30 MYI area export through Fram Strait.
31 3. The Beaufort Sea has become a MYI export pathway rivaling Fram Strait,
32 encouraging the transition to a seasonal Arctic sea ice cover.

33 **Abstract:**

34 Historically multiyear sea ice (MYI) covered a majority of the Arctic and
35 circulated through the Beaufort Gyre for years. However, increased ice melt in the
36 Beaufort Sea during the early-2000s was proposed to have severed this circulation.
37 Constructing a regional MYI budget from 1997-2021 reveals that MYI import into
38 the Beaufort Sea has increased year-round, yet less MYI now survives through
39 summer and is transported onwards in the Gyre. Annual average MYI loss
40 quadrupled over the study period and increased from ~7% to ~33% of annual Fram
41 Strait MYI export, while the peak in 2018 (385,000 km²) was similar in magnitude to
42 Fram Strait MYI export. The ice-albedo feedback coupled with the transition
43 towards younger thinner MYI is responsible for the increased MYI loss. MYI
44 transport through the Beaufort Gyre has not been severed, but it has been reduced
45 so severely to prevent it from being redistributed throughout the Arctic Ocean.

46

47 **Plain Language Summary:**

48 Historically sea ice grew thicker and aged into multiyear sea ice (MYI) as it
49 was transported clockwise around the Beaufort Gyre for up to and beyond 10 years.
50 This pattern facilitated the pan-Arctic distribution of MYI that was typical of the
51 1980s and 1990s. However, warming temperatures and greater sea ice melt in the
52 Beaufort Sea since the early 2000s has significantly increased the annual area of MYI
53 lost to melt, and was proposed to have severed MYI transport through the Beaufort
54 Gyre. Here we use a regional MYI budget to show that an increasing area of MYI is
55 lost annually in the Beaufort Sea and that this has considerably altered and
56 interrupted MYI transport through the Gyre for prolonged periods during recent
57 years. This change has implications regionally for wildlife, shipping, and local
58 communities, while also having an affect on the resiliency of the pan-Arctic ice pack.

59 **1. Introduction:**

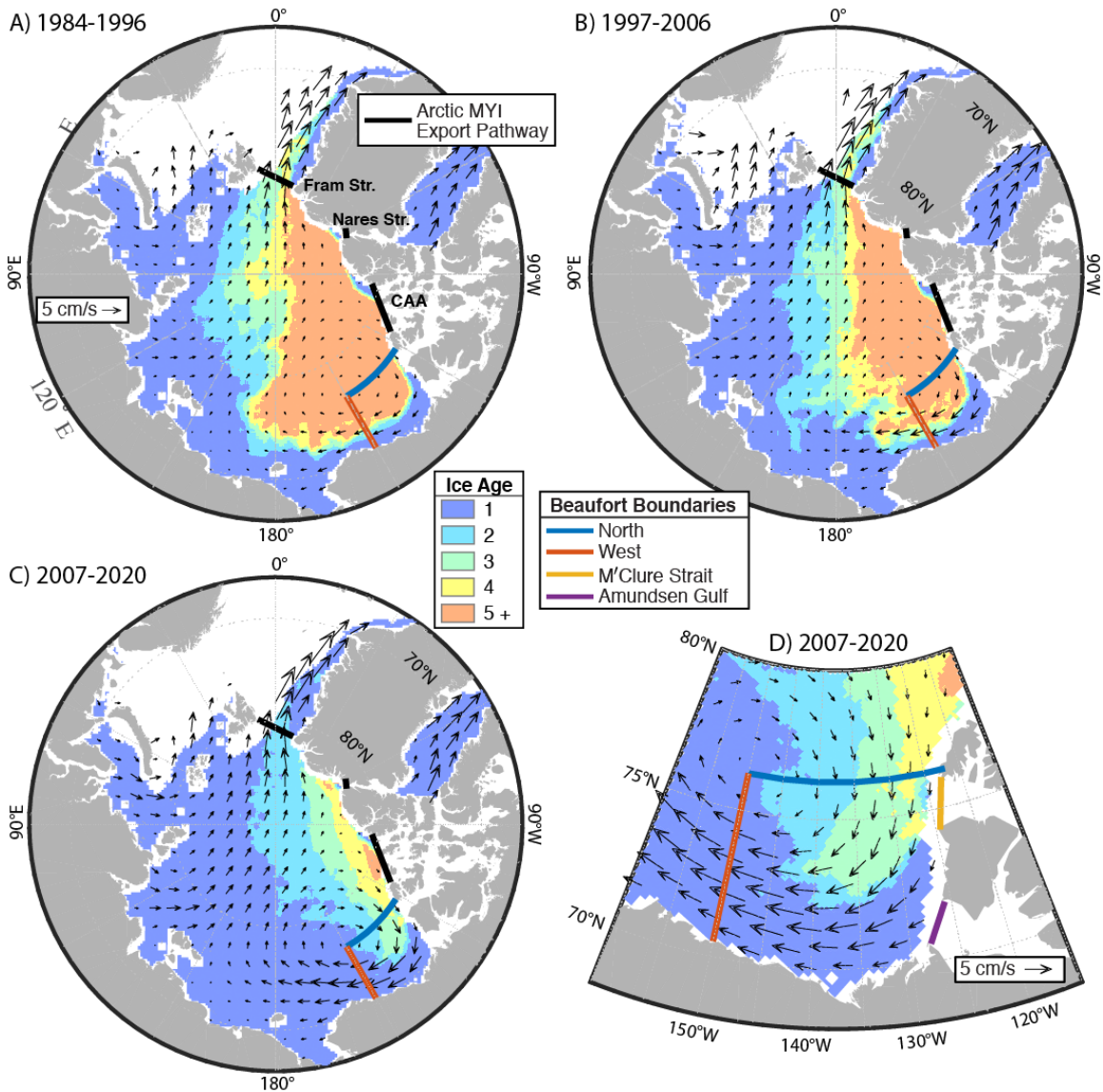
60 Multiyear sea ice (MYI) comprises the thickest and most robust sea ice in the
61 Arctic, however its extent is declining as the Arctic transitions to a predominantly
62 seasonal ice cover (Figure 1; Kwok, 2018). During the 1950s and 1960s, MYI
63 covered the vast majority of the Arctic Ocean ($\sim 5.5 \times 10^6$ km²; Nghiem et al., 2007)
64 and grew thicker as it circulated through the anticyclonic Beaufort Gyre for up to
65 and beyond 10 years (Rigor & Wallace, 2004). Within the Gyre, MYI is transported
66 from the central Arctic, where the thickest and oldest ice is compressed against the
67 northern coast of Greenland and the Canadian Arctic Archipelago (CAA; Bourke &
68 Garret, 1987; Kwok, 2015), through the Beaufort and Chukchi Seas, then onward to
69 the Eastern Arctic. From there MYI is circulated northwards and either retained and
70 recirculated within the Gyre, or entrained in the Transpolar Drift Stream and
71 exported through Fram Strait (Figure 1). The retention of MYI within the Gyre is a
72 critical factor in the mass balance of the Arctic Ocean, as it redistributes MYI
73 throughout the Arctic, maintaining the pan-Arctic distribution of MYI observed
74 throughout the second half of the 20th century (Nghiem et al., 2007) and the start of
75 the observational record in the 1980s (Figure 1A; Maslanik et al., 2011). MYI
76 survival through the Beaufort Sea is key to the process of MYI redistribution
77 because the Beaufort serves as a conduit connecting the central Arctic to the Eastern
78 Arctic. Maslanik et al., (2011) showed that between 1981 and 2005 93% of MYI in
79 the Beaufort Sea survived through summer, which thereby fostered the
80 redistribution of MYI through the Gyre.

81 In 1998, the Beaufort Sea transitioned to a thinner state following anomalous
82 atmospheric forcing and record ice-loss (Hutchings & Rigor, 2012; Maslanik et al.,
83 1999). Since then increased solar heating of the upper ocean and heat transport
84 through the Bering Strait have increased sea ice melt throughout the western Arctic
85 (Planck et al., 2020; Woodgate et al., 2010), particularly bottom melt, of which an
86 extreme amount (2 m) was observed on a MYI floe in the Beaufort Sea during 2007
87 (Perovich et al., 2008). Increased ice melt within the Beaufort Sea has led to reduced
88 summer sea ice extent (Babb et al., 2019), year-round reductions in MYI area (Galley
89 et al., 2016), reductions in MYI thickness (Krishfield et al., 2014), and increased MYI

90 loss, which increased through the 2000s to a peak in 2008 (Kwok & Cunningham,
91 2010). Ultimately, the survival rate of MYI passing through the Beaufort Sea
92 decreased from 93% from 1981-2005 to 73% from 2006-2010 (Maslanik et al.,
93 2011), a change that was further emphasized by the complete loss of the regional
94 MYI pack during summers 2010, 2012 and 2016 (Babb et al., 2016, 2019; Stroeve et
95 al., 2011). However, regardless of MYI loss during summer, the Beaufort Sea
96 continues to be resupplied with MYI from the central Arctic via the Gyre (Figure 1;
97 Babb et al., 2020; Galley et al., 2016; Howell et al., 2016), though less of it is likely to
98 survive through summer. As a result, younger ice is being advected out of the
99 Beaufort Sea (Howell et al., 2016), which has led to younger ice recirculating within
100 the Gyre (Hutchings & Rigor, 2012) and all but eliminated the supply of MYI to the
101 Eastern Arctic, which has predominantly been covered by seasonal ice since 2007
102 (Figure 1C; Kwok, 2018).

103 Based on increased MYI loss in the Beaufort Sea during the early-2000s
104 Maslanik et al. (2007) proposed that the previously continuous journey of MYI
105 through the Beaufort Gyre had been severed and that the western Arctic had
106 become an area of MYI export. In this paper we use 25 years of Canadian Ice Service
107 (CIS) ice charts to present a MYI budget for the Beaufort Sea that accounts for MYI
108 transport and quantifies the annual area of MYI lost to melt in the region from 1997
109 to 2021. We then examine the thermodynamic forcing and dynamic conditioning
110 that is driving the increase in MYI loss and examine MYI loss in the Beaufort Sea
111 relative to MYI export through other pathways. Ultimately, we examine whether
112 MYI transport through the Beaufort Gyre has been severed, leaving the Beaufort Sea
113 as an area of MYI export.

114



115
116 Figure 1: A – C) pan-Arctic fields of mean annual sea ice motion and median ice age
117 during April from 1984-1996, 1997-2006 and 2007-2020. The northern and
118 western boundaries of the Beaufort Sea and other MYI export pathways are
119 presented. D) Mean annual sea ice motion and median ice age during April in the
120 Beaufort Sea from 2007-2020, with the four boundaries of the Beaufort denoted.
121

122 **2. Methods:**

123 To examine the MYI budget of the Beaufort Sea, the region was defined by
124 four boundaries; i) western (150°W), ii) northern (76.25°N), iii) M'Clure Strait and
125 iv) Amundsen Gulf (Figure 1D). The regional MYI area was calculated from ice
126 charts and used to calculate the seasonal change in MYI area during summer (ΔMYI_s ;
127 May through September) and winter (ΔMYI_w ; October through April), while MYI flux

128 (F) across the boundaries was calculated from ice charts and remotely sensed fields
129 of sea ice motion. ΔMYI_w is solely the result of F , while a combination of F and melt
130 dictate ΔMYI_s . Therefore, by calculating the net F during summer we estimate the
131 annual area of MYI lost to melt. MYI area may also be reduced through ice
132 deformation, however following Kwok and Cunningham (2010) this is expected to
133 be very low and is not considered in this budget. The final term in the budget is local
134 MYI replenishment from FYI that survives through summer and becomes classified
135 as MYI on October 1. MYI replenishment is quantified as the regional FYI area in the
136 ice chart from the week prior to October 1.

137 Ice charts delineate different ice regimes with polygons that present the
138 partial concentrations (tenths) of up to three different stages of development
139 according to the World Meteorological Organizations egg code (Fequet, 2005). Since
140 1996, ice charts are created by manually classifying these polygons in RADARSAT
141 images. Within this study we focus on the partial concentration of MYI, which is
142 distinguished from the surrounding FYI types by the tone, texture, and shape within
143 the images (Tivy et al., 2011). Historically, ice charts were produced weekly during
144 summer, and either bi-weekly or monthly during winter. Since 2007 ice charts have
145 been produced weekly year-round. Overall, ice charts provide a consistent, long-
146 term evaluation of the partial concentration of MYI at high resolution. The ice charts
147 are considered more accurate than coarser pan-Arctic fields of ice age derived from
148 lagrangian ice tracking (NSIDC Ice Age; Tschudi et al., 2019), and provide year-
149 round data unlike ice type datasets that are only available seasonally (OSI SAF Sea
150 Ice Type; osi-saf.eumetsat.int). Further details on the ice charts and associated
151 uncertainties are discussed in Tivy et al., (2011).

152 F was calculated at regular intervals along the western (F_W), northern (F_N)
153 and M'Clure (F_M) boundaries using the following equation,

$$154 \quad F = c_{MYI} u \Delta x \quad (1)$$

155 where c_{MYI} is the partial MYI concentration from the ice chart for the corresponding
156 week/month, u is the daily ice velocity component normal to the gate, and Δx is the
157 distance interval (5 km). F was not calculated for Amundsen Gulf because during our
158 study period it has predominantly been covered by FYI (Galley et al., 2016). F_W and

159 F_N were calculated daily using the corresponding ice chart to assess c_{MYI} at each
 160 point, and u from the NSIDC’s Polar Pathfinder ice motion dataset (v4; Tschudi et al.,
 161 2019). However, this dataset does not cover the narrow channels of the CAA, hence
 162 a finer resolution sea ice motion dataset derived from sequential RADARSAT images
 163 (described in Howell & Brady, 2019) was used in conjunction with the ice charts to
 164 quantify monthly values of F_M . Note that F_M is null from November to April due to
 165 landfast ice conditions in M’Clure Strait (Canadian Ice Service, 2011). Across all
 166 three gates positive fluxes represent ice import into the Beaufort Sea, and vice-versa
 167 for negative fluxes. Summing F_N , F_W , and F_M provided the net seasonal F during
 168 summer (1 May to 30 September) and winter (1 October to 30 April), with the
 169 former being used to calculate the annual MYI area lost to melt.

170 The uncertainty in these estimates of MYI lost to melt reflect the uncertainty
 171 in F , which can be estimated with the following equation,

$$172 \quad \sigma_F = \frac{\sigma_e L}{\sqrt{N}} \quad (2)$$

173 where, σ_e is the error in ice drift velocities (km d⁻¹), L is the gate width (km) and N is
 174 the number of samples across the gate. Using this equation and $\sigma_e = 0.43$ km d⁻¹,
 175 Howell et al., (2013) calculated the uncertainty of F_M as 13 km² d⁻¹. σ_e for the NSIDC
 176 ice drift velocities is greater and increases from 1.123 km d⁻¹ between May and
 177 October, to 0.873 km d⁻¹ between November and April (Sumata et al., 2014).
 178 Additionally, σ_e increases with drift speed (Sumata et al., 2015), which may lead to a
 179 bias in underestimating ice flux during periods of high ice drift speeds. With values
 180 of L and N of 715 km and 143 for the northern gate, and 635 km and 127 for the
 181 western gate, the uncertainty in F_N and F_W are 67 and 63 km² d⁻¹ during summer and
 182 52 and 49 km² d⁻¹ during winter. During summer (May 1 – September 30) this
 183 equates to cumulative σ_F in F_N , F_W and F_M of 10,184, 9,576 and 1,976 km²
 184 respectively, or an overall σ_F of 21,736 km² which is approximately 17% of the
 185 average MYI loss (125,000 km²). However, MYI is not present along the entire gate
 186 at all times, so σ_F is lower. Calculating σ_F daily only for points along the northern and
 187 western boundaries where MYI is present, and summing over the melt season, along
 188 with σ_F in F_m , gives a revised σ_F of 18,575 km², or 15% of the average MYI loss.

189 To compliment the MYI budget, several additional datasets were used. The
190 NSIDC Sea Ice Age dataset (v4 - Tschudi et al., 2019a) provides context on the age
191 distribution of MYI within the Beaufort Sea at the end of winter and was used to
192 calculate a second MYI budget that confirms the overall trend of increasing MYI loss
193 in the Beaufort Sea, albeit with a greater magnitude ($-10,000 \text{ km}^2 \text{ yr}^{-1}$; Figure S1).
194 The Pan-Arctic Ice-Ocean Modelling and Assimilation System (PIOMAS; Zhang &
195 Rothrock, 2003) provided estimates of ice thickness along the northern and western
196 boundaries of the Beaufort Sea. Additionally, six-hourly fields of 2 m air
197 temperature and surface solar radiation downwards (SSRD) were retrieved from
198 the ERA-5 reanalysis (Hersbach et al., 2020). Following Perovich et al., (2007; 2008)
199 SSRD was used in combination with daily fields of sea ice concentration (Cavaliere et
200 al., 1996; updated 2021) to estimate solar heating of the upper ocean through areas
201 of open water (F_{ow}). F_{ow} is strongly correlated with bottom melt through the ice-
202 albedo feedback and is associated with both the long-term increase in bottom melt
203 and years of anomalously high ice loss in the Beaufort Sea (Babb et al., 2016, 2019;
204 Perovich et al., 2008, 2011; Planck et al., 2020).

205

206 **3. Results and Discussion:**

207 **3.1 Regional MYI Budget**

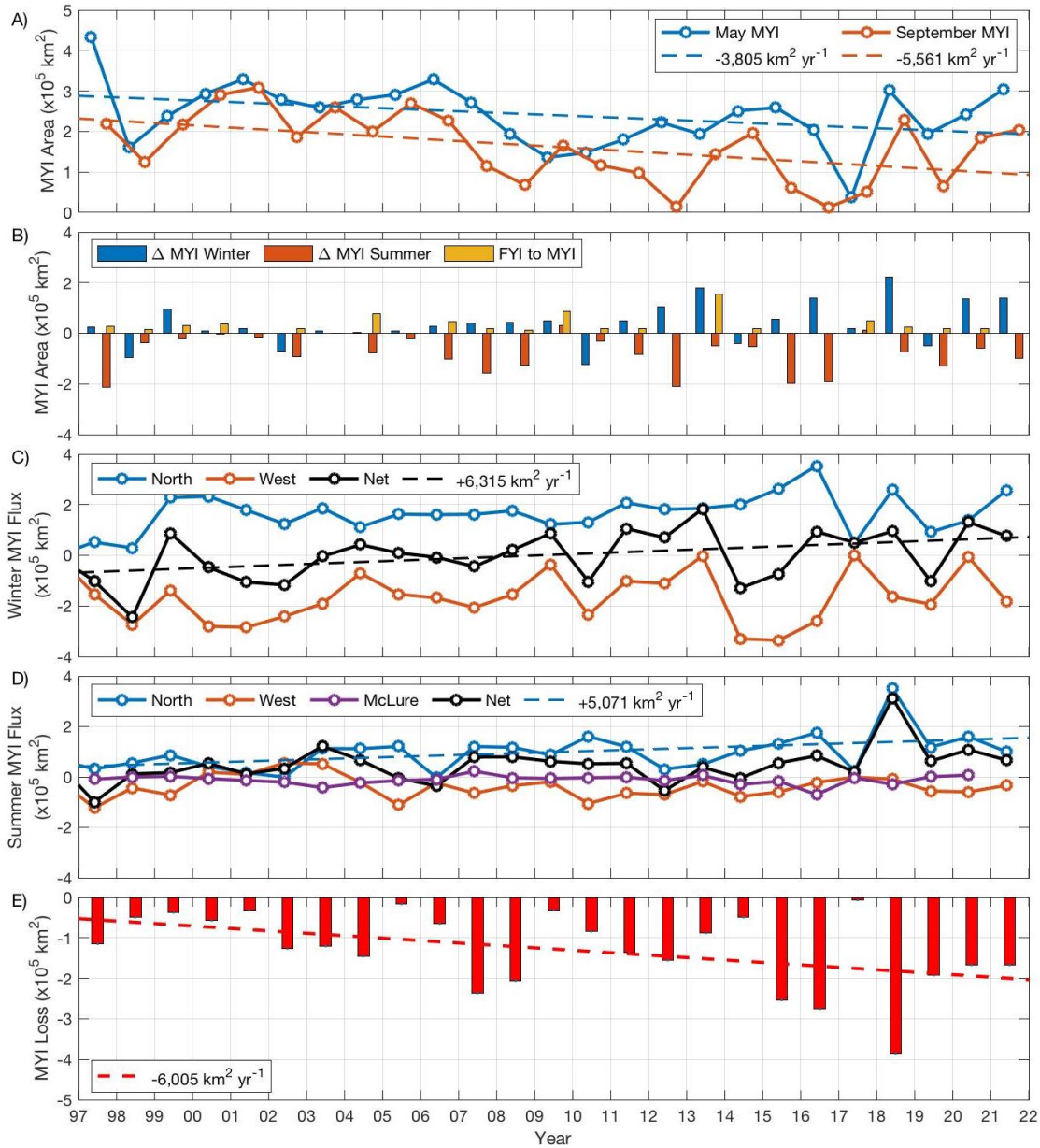
208 From 1997 to 2021 there has been a significant negative trend in MYI area in
209 the Beaufort Sea at the start of May ($-3,805 \text{ km}^2 \text{ yr}^{-1}$) and end of September ($-5,561$
210 $\text{km}^2 \text{ yr}^{-1}$; Figure 2A). The trend in September is $\sim 35\%$ greater than the trend in May,
211 highlighting the tendency towards greater reductions in MYI area during summer
212 and the continued replenishment of MYI via import during winter, which offsets MYI
213 loss from the previous summer (i.e. 2013 and 2018; Figure 2B). Other than import,
214 MYI area can only increase by local MYI replenishment, a process that has been
215 fairly limited over this 25-year period (mean = $28,850 \text{ km}^2$) with the exception of
216 2013 (Figure 2B).

217 In terms of MYI transport, the net seasonal MYI flux varies considerably
218 between years according to the balance of western export and northern import,
219 with transport through M'Clure Strait accounting for only 10% of the summer MYI

220 flux (Figure 2). During winter the average net MYI flux is an export of 4,490 km², but
221 there is considerable interannual variability between import and export. For
222 example, winter export peaked at 245,000 km² in 1998 and preconditioned low ice
223 conditions that summer (Maslanik et al., 1999), while winter import peaked at
224 183,500 km² in 2013 and replenished MYI in the Beaufort Sea following the
225 complete loss of the Beaufort ice pack in summer 2012 (Babb et al., 2016; Figure
226 2C). Underlying the variability in MYI fluxes during winter is a significant positive
227 trend in MYI import (6,315 km² yr⁻¹) that has flipped winter from a period of MYI
228 export at the start of the time series to a period of MYI import and replenishment
229 more recently (Figure 2C).

230 During summer, an average of 47,120 km² of MYI is imported into the
231 Beaufort Sea (Figure 2D). Summer export peaked at 99,430 km² in 1997 and
232 contributed to the dramatic regional loss of MYI prior to the 1998 minimum, while
233 summer import peaked at 312,670 km² in 2018, and was solely the result of
234 northern import. From 1997-2021, there has been a significant positive trend in
235 northern MYI import during summer (5,071 km² yr⁻¹; Figure 2D).

236 Overall, from 1997-2021, MYI transport through the Beaufort Sea was highly
237 variable, but significant trends towards greater MYI import year-round have been
238 loading MYI from the central Arctic into the Beaufort. However, less of this MYI is
239 surviving through summer. From 1997-2021, an average of 125,000 km² of MYI
240 area was lost in the Beaufort Sea each summer. The minimum loss occurred in 2017,
241 when very little MYI was present in the Beaufort following the reversal of the
242 Beaufort Gyre (Babb et al., 2020), while the maximum loss (385,000 km²) occurred
243 in 2018, though record northern import maintained a peak in regional MYI area
244 during September 2018 (Figure 2). Between 1997-2021 there was a significant
245 increase in MYI loss in the Beaufort Sea (-6,005 km² yr⁻¹; Figure 2E). The fact that
246 the trends in MYI loss and September MYI area (-5,561 km² yr⁻¹) are similar,
247 coupled with a non-significant trend in net MYI transport during summer, indicates
248 that melt, not transport, is driving the increase in MYI loss in the Beaufort Sea.

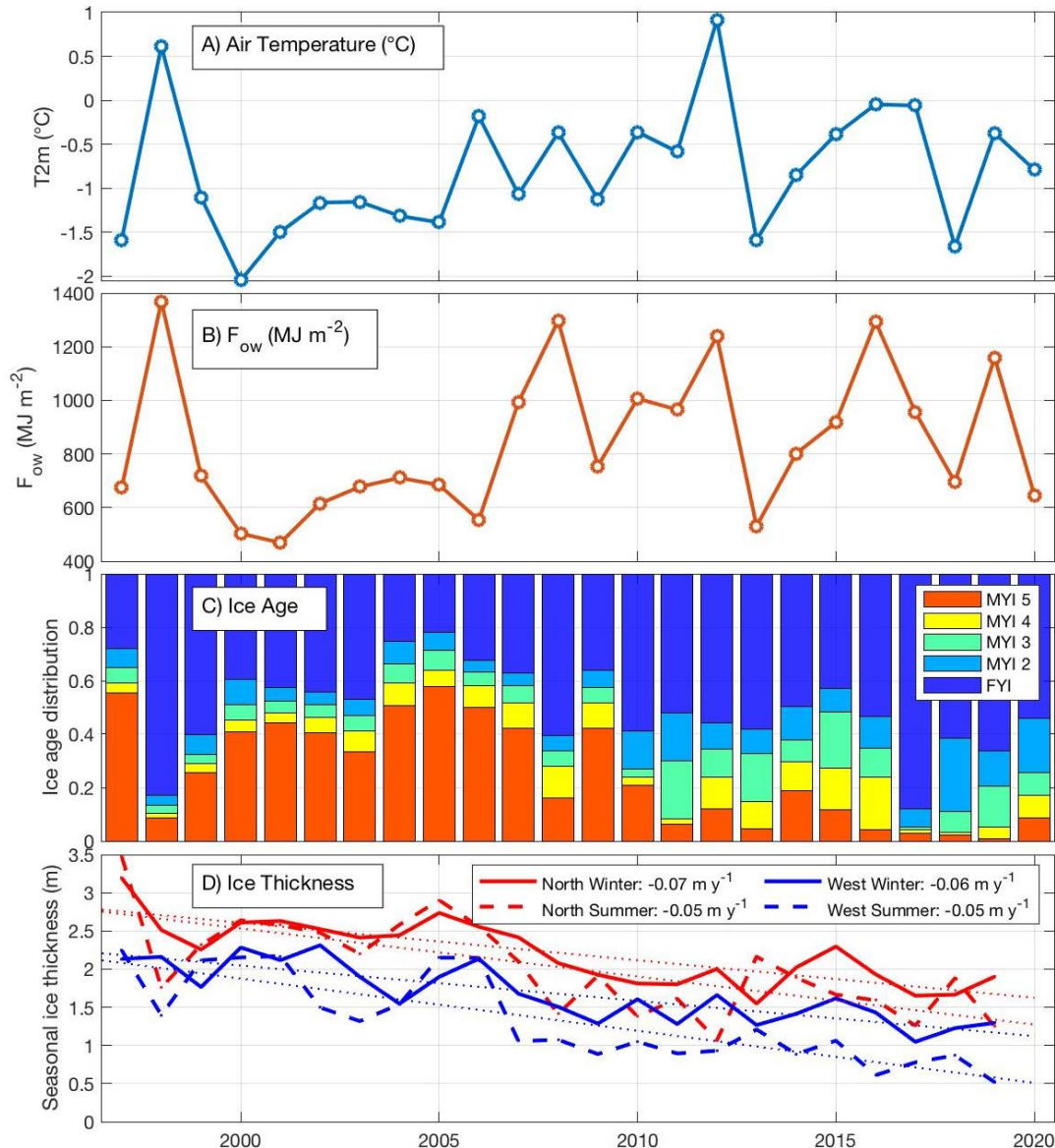


249
250 Figure 2: Annual time series of the MYI budget from 1997 to 2021. A) Regional MYI
251 area during May and September. B) Seasonal changes in MYI area during winter and
252 summer, and MYI replenishment during October. Seasonal MYI fluxes during winter
253 (C) and summer (D) across the northern, western and M'Clure boundaries, along
254 with the net seasonal MYI flux. E) MYI area loss in the Beaufort Sea. Dashed lines
255 denote significant ($p < 0.05$) trends.
256

257 **3.2 Thermodynamic forcing and dynamic conditioning of MYI loss**

258 MYI loss is not a new phenomenon in the Beaufort Sea, though between 1981
259 and 2005 only 7% of MYI in the western Arctic melted out each summer (Maslanik
260 et al., 2011). The recent increase in MYI loss reflects a balance of factors that either

261 drive ice melt (i.e. air temperatures, and the ice-albedo feedback) or dictate the
262 condition and therefore the resiliency of the ice pack entering the melt season (i.e.
263 thickness and age). Examining these factors over the same period as the budget
264 reveals non-significant increases in air temperatures and F_{ow} during summer, with
265 notable peaks during years of regional sea ice minima (1998, 2008, 2012 and 2016;
266 Figure 3) during which MYI loss also peaked (Figure 2E). At the same time, the
267 presence of MYI in the Beaufort Sea has not only declined, but the age of the MYI has
268 decreased, with a dramatic loss of MYI 5+ years old since 2010 (Figure 3C). This
269 accompanies a negative trend in ice thickness along the northern gate during both
270 winter and summer (Figure 3D). Interestingly, the peak in MYI loss during 2018
271 does not correspond to anomalously warm air temperatures or increased F_{ow} during
272 summer, but rather to an end-of-winter ice pack that was very young, with a
273 majority of the MYI being only 2 years old (Figure 3) and in part created by low ice
274 conditions during the two preceding summers (Babb et al., 2019; 2020). Overall, the
275 Beaufort ice pack has been getting progressively younger, thinner, and therefore
276 less resilient, while it has also been exposed to warmer air temperatures and a
277 stronger ice-albedo feedback.



278
279 Figure 3: Time series of the thermodynamic and dynamic factors that either drive
280 melt or condition the ice pack. Mean air temperature (A) and cumulative F_{ow} (B)
281 over the Beaufort Sea from May through September. C) Distribution of ice age within
282 the Beaufort Sea at the end of April. D) Mean seasonal ice thickness along the
283 northern and western boundaries during winter and summer. Significant trends (p
284 < 0.05) are presented with dotted lines.
285

286 **3.3 Has MYI loss severed MYI transport within the Beaufort Gyre?**

287 From 1997-2020, an average of 200,000 km² of MYI was exported from the
288 Beaufort Sea across the western gate annually. However, western export is highly
289 variable, and ranged from a maximum export of 406,000 km² in 2014 following the
290 recovery of MYI in 2013, to a net import of 750 km² in 2017 as a result of the

291 Beaufort Gyre reversal (Babb et al., 2020). Strong variability in MYI export
292 precludes significant trends, although during four recent winters essentially no MYI
293 was exported across the gate (2009, 2013, 2017 and 2020; Figure 2C). Furthermore,
294 there is a significant positive trend in FYI export across the western gate (11,300
295 km² yr⁻¹), indicating younger ice is being exported into the Chukchi Sea in place of
296 MYI.

297 Whilst there has not been a significant trend in MYI export across the
298 western gate, there has been a decrease in the thickness and physical character of
299 MYI exported across the gate. At the end of summer 2009 the remnant MYI in the
300 western Beaufort Sea was heavily deteriorated and isothermal (Barber et al., 2009),
301 while since 2007 remnant MYI has been so thin that by the end of the following
302 winter it is as thick as the surrounding FYI (Mahoney et al., 2019). Furthermore,
303 there are significant negative trends in sea ice thickness along the western gate
304 during summer and winter that equate to approximately 1.5 m over the study
305 period (Figure 3).

306 MYI transport through the Beaufort Sea as part of the Beaufort Gyre has not
307 been totally severed. However, it has been interrupted and reductions in the area,
308 thickness and age of MYI transported downstream into the Chukchi Sea have made
309 that ice pack more vulnerable to warm pacific waters flowing through the Bering
310 Strait (Woodgate et al., 2010) and the ice-albedo feedback (Serreze et al., 2016).

311

312 **3.4 Has the Beaufort Sea become an area of MYI export?**

313 Traditionally, MYI export occurs along the boundaries of the Arctic Ocean
314 and represents the total loss of MYI. Fram Strait is the primary export pathway
315 (Kwok, 2009) exporting between 450,000 and 660,000 km² of MYI annually (Table
316 1). MYI is also exported annually through Nares Strait and into the Queen Elizabeth
317 Islands (QEI; Howell & Brady, 2019; Kwok, 2005, 2006; Moore et al., 2021), and has
318 occasionally been exported into the Barents Sea (Kwok, 2004) and through the
319 Bering Strait (Babb et al., 2013). In order to define the Beaufort Sea as an export
320 pathway similar to these other locations the regional MYI pack would have to be
321 completely lost. This has happened three times during the last decade (2010, 2012,

2016). But as we have just shown, younger and thinner MYI does continue to be advected downstream within the Gyre. Hence, the Beaufort Sea has not completely become an export pathway, but it increasingly resembles one.

Comparing MYI loss in the Beaufort to MYI export through the traditional export pathways reveals that during the first pentad of our budget (1997-2001) MYI loss in the Beaufort was approximately twice the net MYI export through Nares Strait and into the QEI, but only 6% to 9% of the MYI export through Fram Strait (Table 1). Comparatively, during the most recent pentad (2017-2021) MYI loss in the Beaufort Sea was approximately three times the net MYI export through Nares Strait and into the QEI, and approximately 27% to 40% of the annual MYI export through Fram Strait (Table 1). Furthermore, the 2018 peak in MYI loss (385,000 km²) was close to the conservative estimate of MYI export through Fram Strait.

Without estimates of MYI loss in other regions it is not possible to compare sub-regional MYI loss to the overall pan-Arctic annual MYI loss (melt + export). Although this comparison shows that amongst these four pathways of MYI loss, the Beaufort Sea continues to have the second greatest magnitude, and that its relative contribution to the Arctic MYI balance has significantly increased. This increase is critical for the MYI that remains in the central Arctic, as it is now bookended by Fram Strait and the Beaufort Sea (Figure 1) and is susceptible to being lost through either side. Historically, MYI advected from the central Arctic through the Beaufort Gyre was conserved, particularly during a negative phase of the Arctic Oscillation when a large Beaufort Gyre retained ice within the western Arctic (Rigor et al., 2002; Stroeve et al., 2011). However, increasing MYI loss in the Beaufort Sea limits the potential of the Gyre to retain MYI and facilitate a recovery. As an example, during winter 2021 a strong Beaufort High advected MYI out of the central Arctic into the Beaufort Sea (Mallett et al., 2021), and while this facilitated a slight recovery in the regional MYI area (Figure 2A), over 170,000 km² of this MYI was lost (Figure 2E) and we speculate that the remaining MYI was heavily deteriorated.

Ultimately, the combination of increasing MYI loss in the Beaufort Sea (Figure 2E), increasing MYI export through Nares Strait (Moore et al., 2021) and into the QEI (Howell & Brady, 2019), and continued MYI export through Fram Strait

353 is depleting the reservoir of MYI in the Arctic Ocean. This trend is compounded by a
354 concomitant decrease in MYI replenishment by FYI (Kwok, 2007). The imbalance
355 between MYI loss (melt and export) and MYI replenishment from FYI is driving the
356 transition to a predominantly seasonal ice cover that is inherently thinner and will
357 eventually lead to the occurrence of a seasonally ice-free Arctic (SIMIP, 2020).

358

359 Table 1: Comparison of MYI loss in the Beaufort Sea to MYI export through export
360 pathways.

	Years			Annual MYI loss
MYI loss in the Beaufort Sea	1997-2001			42,360 km ²
	2017-2021			183,250 km ²
Export Pathway	Years	Annual ice export	Proportion MYI	Annual MYI loss
Fram Strait	1979-2007	706,000 km ² (a)	64-94% (b)	451,000 – 663,000 km ²
Nares Strait	1996-2002	33,000 km ² (c)	50% (c)	16,500 km ²
	2019-2021	87,000 km ² (d)	50% (c)	43,500 km ²
QEI	1997-2002	8,000 km ² (e)	100%*	8,000 km ²
	1997-2018	25,000 km ² (f)	100%*	25,000 km ²

361 Notes: a – Kwok (2009); b – Ricker et al., (2018); c – Kwok, (2005); d – Moore et al.,
362 (2021); e – Kwok, (2006); f – Howell & Brady (2019).

363 * Estimated based on the CIS ice charts.

364

365 **3.5 The impacts of increasing MYI loss in the Beaufort Sea**

366 The loss of MYI has various impacts on the way that humans and wildlife
367 interact with the ice pack within the Beaufort Sea. Given its thickness, and strength,
368 MYI represents a considerable hazard to vessels operating in ice-covered waters.
369 The reduction in MYI area within the Beaufort Sea corresponds to an increase in
370 shipping activity (Pizzolato et al., 2016), particularly pleasure craft that are
371 accessing the Northwest Passage (Dawson et al., 2018). Shipping in the Beaufort Sea
372 is proposed to continue to increase as the shipping season length continues to

373 increase (Mudryk et al., 2021). However, the continued replenishment of MYI during
374 winter will maintain some level of risk associated with hazardous ice (Barber et al.,
375 2014).

376 The transition to a thinner seasonal ice pack is projected to increase
377 productivity in the Arctic (Tedesco et al., 2019) and has been proposed to offer
378 some short-term benefits to Polar Bears (Derocher et al., 2004). However, Laidre et
379 al., (2020) noted that this has yet to be demonstrated and suggest any advantage
380 may only be temporary before the negative effects of climate change (i.e. habitat
381 loss) begin to outweigh any potential positives. Historically, Polar Bears within the
382 Beaufort Sea retreated to the MYI pack during summer (Derocher et al., 2004) and
383 even denned on MYI floes during winter (Amstrup & Gardner, 1994). But MYI loss
384 combined with the northern retreat of the MYI edge (Galley et al., 2016), is both
385 removing and fragmenting this habitat and increasing the distance that bears may
386 need to swim to reach either the remaining MYI or land (Pagano et al., 2021).

387

388 **4. Conclusions:**

389 Historically, the Beaufort Sea served as a conduit for MYI transport from the
390 central Arctic to the Eastern Arctic through the Beaufort Gyre, and thereby
391 facilitated the pan-Arctic distribution of MYI. However, increasing ice melt during
392 the early-2000s led Maslanik et al. (2007) to propose that the Beaufort Sea had
393 become an area of MYI export and that MYI transport through the Beaufort Gyre had
394 been severed. Using a regional MYI budget from 1997-2021, we determined that
395 MYI transport through the Beaufort Sea has not been completely severed, but that it
396 has been interrupted and essentially now provides no replenishment of MYI to the
397 Eastern Arctic. The budget reveals that MYI import into the Beaufort Sea has
398 increased during both summer and winter, but that less of this MYI now survives
399 through summer. Over the 25-year study period, MYI area loss increased at 6,289
400 km² yr⁻¹, nearly quadrupling the annual mean area of MYI lost from 42,360 km²
401 between 1997-2001 to 183,000 km² between 2017-2021. MYI area loss peaked at
402 385,000 km² in 2018.

403 Historically, the pan-Arctic MYI budget was dominated by MYI loss through
404 Fram Strait. At the start of the record, MYI loss in the Beaufort Sea represented only
405 7% of the annual MYI export through Fram Strait. However, from 2017-2021 this
406 increased to ~35%, with the peak in 2018 matching the conservative estimate of
407 MYI export through Fram Strait (~400,000 km²). This increase in MYI loss in the
408 Beaufort Sea has been driven by a combination of thermodynamic forcing and
409 dynamic conditioning, which have collectively exposed a younger, thinner ice pack
410 to warmer air temperatures and a stronger ice-albedo feedback. Increased MYI loss
411 has interrupted MYI transport through the Gyre, leading to a deteriorated form of
412 MYI being advected downstream. Ultimately, the contribution of MYI loss in the
413 Beaufort Sea to the overall MYI budget of the Arctic Ocean has dramatically
414 increased and is a key driver of the transition to a seasonal Arctic ice pack.

415 **Acknowledgements:**

416 D. Babb, R. Galley and D. Barber would like to acknowledge the financial
417 support from the Natural Sciences and Engineering Research Council of Canada
418 (NSERC). Thanks to the Canada Research Chair (CRC), Canada Excellence Research
419 Chair (CERC) and the Canada-150 Chair (C-150) programs. D. Babb acknowledges
420 financial support from the Canadian Meteorological and Oceanographic Society
421 (CMOS). J. Landy acknowledges support from the Centre for Integrated Remote
422 Sensing and Forecasting for Arctic Operations (CIRFA) project through the Research
423 Council of Norway (RCN) under Grant #237906. J. Landy and J. Stroeve acknowledge
424 support from the Natural Environment Research Council Project “PRE-MELT” under
425 Grant NE/T000546/1. We would also like to thank the editor and two anonymous
426 reviewers for their help in improving this manuscript.

427

428 **Data Availability**

429 CIS ice charts are freely available online ([https://www.canada.ca/en/environment-](https://www.canada.ca/en/environment-climate-change/services/ice-forecasts-observations.html)
430 [climate-change/services/ice-forecasts-observations.html](https://www.canada.ca/en/environment-climate-change/services/ice-forecasts-observations.html)). The NSIDC ice motion
431 (<https://nsidc.org/data/nsidc-0116/versions/4>) and ice age
432 (<https://nsidc.org/data/NSIDC-0611/versions/4>) datasets are available online.
433 PIOMAS Ice thickness data is available online
434 ([http://psc.apl.uw.edu/research/projects/arctic-sea-ice-volume-](http://psc.apl.uw.edu/research/projects/arctic-sea-ice-volume-anomaly/data/model_grid)
435 [anomaly/data/model_grid](http://psc.apl.uw.edu/research/projects/arctic-sea-ice-volume-anomaly/data/model_grid)). ERA5 atmospheric reanalysis products are available
436 from the Climate Data Store through the Copernicus Climate Change Service
437 ([https://cds.climate.copernicus.eu/cdsapp#!/dataset/reanalysis-era5-single-](https://cds.climate.copernicus.eu/cdsapp#!/dataset/reanalysis-era5-single-levels?tab=overview)
438 [levels?tab=overview](https://cds.climate.copernicus.eu/cdsapp#!/dataset/reanalysis-era5-single-levels?tab=overview)).

439 **References:**

- 440 Amstrup, S. C., & Gardner, C. L. (1994). Polar bear maternity denning in the Beaufort
441 Sea. *Journal of Wildlife Management*, 58(1), 1–10.
442 <https://doi.org/10.2307/3809542>
- 443 Babb, D.G., Landy, J. C., Lukovich, J. V., Haas, C., Hendricks, S., Barber, D. G., & Galley,
444 R. J. (2020). The 2017 reversal of the Beaufort Gyre: Can dynamic thickening of
445 a seasonal ice cover during a reversal limit summer ice melt in the Beaufort
446 Sea? *Journal of Geophysical Research: Oceans*, 1–26.
447 <https://doi.org/10.1029/2020jc016796>
- 448 Babb, David G., Galley, R. J., Asplin, M. G., Lukovich, J. V., & Barber, D. G. (2013).
449 Multiyear sea ice export through the Bering Strait during winter 2011-2012.
450 *Journal of Geophysical Research: Oceans*, 118(10), 5489–5503.
451 <https://doi.org/10.1002/jgrc.20383>
- 452 Babb, David G., Galley, R. J., Barber, D. G., & Rysgaard, S. (2016). Physical processes
453 contributing to an ice free Beaufort Sea during September 2012. *Journal of*
454 *Geophysical Research: Oceans*, 121, 267–283.
455 <https://doi.org/10.1002/2015JC010756>
- 456 Babb, David G., Landy, J. C., Barber, D. G., & Galley, R. J. (2019). Winter Sea Ice Export
457 From the Beaufort Sea as a Preconditioning Mechanism for Enhanced Summer
458 Melt: A Case Study of 2016. *Journal of Geophysical Research: Oceans*,
459 1998(6575), 6575–6600. <https://doi.org/10.1029/2019JC015053>
- 460 Barber, D. G., Galley, R. J., Asplin, M. G., De Abreu, R., Warner, K. A., Pučko, M., et al.
461 (2009). Perennial pack ice in the southern beaufort sea was not as it appeared
462 in the summer of 2009. *Geophysical Research Letters*, 36(24), 1–5.
463 <https://doi.org/10.1029/2009GL041434>
- 464 Barber, D. G., McCullough, G., Babb, D. G., Komarov, A., Candlish, L. M., Lukovich, J. V.,
465 et al. (2014). Climate change and ice hazards in the Beaufort Sea. *Elementa:*
466 *Science of the Anthropocene*, 2(1982), 000025.
467 <https://doi.org/10.12952/journal.elementa.000025>
- 468 Bourke, R. H., & Garret, R. P. (1987). Sea ice thickness distribution in the Arctic
469 Ocean. *Cold Regions Science and Technology*, 13, 259–280.
- 470 Canadian Ice Service. (2011). *Sea Ice Climatic Atlas for the Northern Canadian Waters*
471 *1981-2011*. Ottawa, Canada.
- 472 Cavalieri, D. J., Parkinson, C. L., Gloersen, P., & Zwally, H. J. (1996). *Sea Ice*
473 *Concentrations from Nimbus-7 SMMR and DMSP SSM/I-SSMIS Passive Microwave*
474 *Data*. Boulder, Colorado, USA.
- 475 Dawson, J., Pizzolato, L., Howell, S. E. L., Copland, L., & Johnston, M. E. (2018).
476 Temporal and Spatial Patterns of Ship Traffic in the Canadian Arctic from 1990
477 to 2015 + Supplementary Appendix 1: Figs. S1–S7 (See Article Tools). *Arctic*,
478 71(1), 15. <https://doi.org/10.14430/arctic4698>
- 479 Derocher, A. E., Lunn, N. J., & Stirling, I. (2004). Polar Bears in a Warming Climate.
480 *Integrative and Comparative Biology*, 44(2), 163–176.
481 <https://doi.org/10.1093/icb/44.2.163>
- 482 Fequet, D. (2005). *Manual of Standard Procedures for Observing and Reporting Ice*
483 *Conditions* (9th ed.). Ottawa: Canadian Ice Service, Environment Canada.

- 484 Galley, R. J., Babb, D. G., Ogi, M., Else, B. G. T., Geifus, N. X., Crabeck, O., et al. (2016).
485 Replacement of multiyear sea ice and changes in the open water season
486 duration in the Beaufort Sea since 2004. *Journal of Geophysical Research:*
487 *Oceans*, 121(April), 1–18. <https://doi.org/10.1002/2015JC011583>. Received
488 Hersbach, H., Bell, B., Berrisford, P., Hirahara, S., Horányi, A., Muñoz-Sabater, J., et al.
489 (2020). The ERA5 global reanalysis. *Quarterly Journal of the Royal*
490 *Meteorological Society*, 146(730), 1999–2049.
491 <https://doi.org/https://doi.org/10.1002/qj.3803>
492 Howell, S. E. L., & Brady, M. (2019). The Dynamic Response of Sea Ice to Warming in
493 the Canadian Arctic Archipelago. *Geophysical Research Letters*, 46(22), 13119–
494 13125. <https://doi.org/10.1029/2019GL085116>
495 Howell, S. E. L., Brady, M., Derksen, C., & Kelly, R. E. J. (2016). Recent changes in sea
496 ice area flux through the Beaufort Sea during the summer. *Journal of*
497 *Geophysical Research: Oceans*, 121, 1–14.
498 <https://doi.org/10.1002/2015JC011464>
499 Hutchings, J. K., & Rigor, I. G. (2012). Role of ice dynamics in anomalous ice
500 conditions in the Beaufort Sea during 2006 and 2007. *Journal of Geophysical*
501 *Research: Oceans*, 117(5), 1–14. <https://doi.org/10.1029/2011JC007182>
502 Krishfield, R. A., Proshutinsky, A., Tateyama, K., Williams, W. J., Carmack, E. C.,
503 McLaughlin, F. A., & Timmermans, M.-L. (2014). Deterioration of perennial sea
504 ice in the Beaufort Gyre from 2003 to 2012 and its impact on the oceanic
505 freshwater cycle. *Journal of Geophysical Research: Oceans*, 119, 35.
506 <https://doi.org/10.1002/2013JC008999>
507 Kwok, R. (2004). Fram Strait sea ice outflow. *Journal of Geophysical Research*,
508 109(C1), C01009. <https://doi.org/10.1029/2003JC001785>
509 Kwok, R. (2005). Variability of Nares Strait ice flux. *Geophysical Research Letters*,
510 32(24), 1–4. <https://doi.org/10.1029/2005GL024768>
511 Kwok, R. (2006). Exchange of sea ice between the Arctic Ocean and the Canadian
512 Arctic Archipelago. *Geophysical Research Letters*, 33(16), 1–5.
513 <https://doi.org/10.1029/2006GL027094>
514 Kwok, R. (2007). Near zero replenishment of the Arctic multiyear sea ice cover at
515 the end of 2005 summer. *Geophysical Research Letters*, 34(5), 1–6.
516 <https://doi.org/10.1029/2006GL028737>
517 Kwok, R. (2009). Outflow of Arctic Ocean sea ice into the Greenland and Barent Seas:
518 1979-2007. *Journal of Climate*, 22(9), 2438–2457.
519 <https://doi.org/10.1175/2008JCLI2819.1>
520 Kwok, R. (2015). Sea ice convergence along the Arctic coasts of Greenland and the
521 Canadian Arctic Archipelago: Variability and extremes (1992-2014).
522 *Geophysical Research Letters*, 42, 1–8. <https://doi.org/10.1002/2015GL065462>
523 Kwok, R. (2018). Arctic sea ice thickness, volume, and multiyear ice coverage: losses
524 and coupled variability (1958 – 2018). *Environmental Research Letters*, 13(10),
525 105005. <https://doi.org/10.1088/1748-9326/aae3ec>
526 Kwok, R., & Cunningham, G. F. (2010). Contribution of melt in the Beaufort Sea to the
527 decline in Arctic multiyear sea ice coverage: 1993-2009. *Geophysical Research*
528 *Letters*, 37(20), 1–5. <https://doi.org/10.1029/2010GL044678>
529 Laidre, K. L., Atkinson, S. N., Regehr, E. V., Stern, H. L., Born, E. W., Wiig, Ø., et al.

- 530 (2020). Transient benefits of climate change for a high-Arctic polar bear (*Ursus*
531 *maritimus*) subpopulation. *Global Change Biology*, 26(11), 6251–6265.
532 <https://doi.org/https://doi.org/10.1111/gcb.15286>
- 533 Mahoney, A. R., Hutchings, J. K., Eicken, H., & Haas, C. (2019). Changes in the
534 Thickness and Circulation of Multiyear Ice in the Beaufort Gyre Determined
535 From Pseudo-Lagrangian Methods from 2003–2015. *Journal of Geophysical*
536 *Research: Oceans*, 124(8), 5618–5633. <https://doi.org/10.1029/2018JC014911>
- 537 Mallett, R. D. C., Stroeve, J. C., Cornish, S. B., Crawford, A. D., Lukovich, J. V., Serreze,
538 M. C., et al. (2021). Record winter winds in 2020/21 drove exceptional Arctic
539 sea ice transport. *Communications Earth & Environment*, 2(1), 17–22.
540 <https://doi.org/10.1038/s43247-021-00221-8>
- 541 Maslanik, J. A., Serreze, M. C., & Agnew, T. (1999). On the record reduction in 1998
542 Western Arctic sea-ice cover. *Geophysical Research Letters*, 26(13), 1905–1908.
543 <https://doi.org/10.1029/1999GL900426>
- 544 Maslanik, J. A., Fowler, C., Stroeve, J. C., Drobot, S., Zwally, J., Yi, D., & Emery, W.
545 (2007). A younger, thinner Arctic ice cover: Increased potential for rapid,
546 extensive sea-ice loss. *Geophysical Research Letters*, 34(24), 2004–2008.
547 <https://doi.org/10.1029/2007GL032043>
- 548 Maslanik, J. A., Stroeve, J. C., Fowler, C., & Emery, W. (2011). Distribution and trends
549 in Arctic sea ice age through spring 2011. *Geophysical Research Letters*, 38(13),
550 2–7. <https://doi.org/10.1029/2011GL047735>
- 551 Moore, G. W. K., Howell, S. E. L., Brady, M., Xu, X., & McNeil, K. (2021). Anomalous
552 collapses of Nares Strait ice arches leads to enhanced export of Arctic sea ice.
553 *Nature Communications*, 12(1), 1–8. [https://doi.org/10.1038/s41467-020-](https://doi.org/10.1038/s41467-020-20314-w)
554 [20314-w](https://doi.org/10.1038/s41467-020-20314-w)
- 555 Mudryk, L. R., Dawson, J., Howell, S. E. L., Derksen, C., Zagon, T. A., & Brady, M.
556 (2021). Impact of 1, 2 and 4 °C of global warming on ship navigation in the
557 Canadian Arctic. *Nature Climate Change*, 29–31.
558 <https://doi.org/10.1038/s41558-021-01087-6>
- 559 Nghiem, S. V., Rigor, I. G., Perovich, D. K., Clemente-Colón, P., Weatherly, J. W., &
560 Neumann, G. (2007). Rapid reduction of Arctic perennial sea ice. *Geophysical*
561 *Research Letters*, 34(19), 1–6. <https://doi.org/10.1029/2007GL031138>
- 562 Pagano, A. M., Durner, G. M., Atwood, T. C., & Douglas, D. C. (2021). Effects of sea ice
563 decline and summer land use on polar bear home range size in the Beaufort
564 Sea. *Ecosphere*, 12(10). <https://doi.org/10.1002/ecs2.3768>
- 565 Perovich, D. K., Richter-Menge, J. A., Jones, K. F., & Light, B. (2008). Sunlight, water,
566 and ice: Extreme Arctic sea ice melt during the summer of 2007. *Geophysical*
567 *Research Letters*, 35(11), 2–5. <https://doi.org/10.1029/2008GL034007>
- 568 Perovich, D. K., Richter-Menge, J. A., Jones, K. F., Light, B., Elder, B. C., Polashenski, C.,
569 et al. (2011). Arctic sea-ice melt in 2008 and the role of solar heating. *Annals of*
570 *Glaciology*, 52(57 PART 2), 355–359.
571 <https://doi.org/10.3189/172756411795931714>
- 572 Pizzolato, L., Howell, S. E. L., Dawson, J., Laliberté, F., & Copland, L. (2016). The
573 influence of declining sea ice on shipping activity in the Canadian Arctic.
574 *Geophysical Research Letters*, 43(23), 12,146–12,154.
575 <https://doi.org/10.1002/2016GL071489>

- 576 Planck, C. J., Perovich, D. K., & Light, B. (2020). A Synthesis of Observations and
577 Models to Assess the Time Series of Sea Ice Mass Balance in the Beaufort Sea.
578 *Journal of Geophysical Research: Oceans*, 1–15.
579 <https://doi.org/10.1029/2019jc015833>
- 580 Ricker, R., Girard-Ardhuin, F., Krumpfen, T., & Lique, C. (2018). Satellite-derived sea
581 ice export and its impact on Arctic ice mass balance. *The Cryosphere*, 12(9),
582 3017–3032. <https://doi.org/10.5194/tc-12-3017-2018>
- 583 Rigor, I. G., & Wallace, J. M. (2004). Variations in the age of Arctic sea-ice and
584 summer sea-ice extent. *Geophysical Research Letters*, 31(9), 2–5.
585 <https://doi.org/10.1029/2004GL019492>
- 586 Rigor, I. G., Wallace, J. M., & Colony, R. L. (2002). Response of sea ice to the Arctic
587 Oscillation. *Journal of Climate*, 15, 2648–2663. [https://doi.org/10.1175/1520-0442\(2002\)015<2648:ROSITT>2.0.CO;2](https://doi.org/10.1175/1520-0442(2002)015<2648:ROSITT>2.0.CO;2)
- 589 Serreze, M. C., Crawford, A. D., Stroeve, J. C., Barrett, A. P., & Woodgate, R. A. (2016).
590 Variability, trends, and predictability of seasonal sea ice retreat and advance in
591 the Chukchi Sea. *Journal of Geophysical Research: Oceans*, 121, 7308–7325.
592 <https://doi.org/10.1002/2016JC011977>
- 593 SIMIP Community. (2020). Arctic Sea Ice in CMIP6. *Geophysical Research Letters*,
594 47(10). <https://doi.org/10.1029/2019gl086749>
- 595 Stroeve, J. C., Maslanik, J. A., Serreze, M. C., Rigor, I. G., Meier, W., & Fowler, C. (2011).
596 Sea ice response to an extreme negative phase of the Arctic Oscillation during
597 winter 2009/2010. *Geophysical Research Letters*, 38(2), 1–6.
598 <https://doi.org/10.1029/2010GL045662>
- 599 Sumata, H., Lavergne, T., Girard-Ardhuin, F., Kimura, N., Tschudi, M. A., Kauker, F., et
600 al. (2014). An intercomparison of Arctic ice drift products to deduce
601 uncertainty estimates. *Journal of Geophysical Research: Oceans*, 119, 4887–4921.
602 <https://doi.org/10.1002/2013JC009724>
- 603 Sumata, H., Kwok, R., Gerdes, R., Kauker, F., & Karcher, M. (2015). Uncertainty of
604 Arctic summer ice drift assessed by high-resolution SAR data. *Journal of*
605 *Geophysical Research: Oceans*, 120(8), 5285–5301.
606 <https://doi.org/10.1002/2015JC010810>
- 607 Tedesco, L., Vichi, M., & Scoccimarro, E. (2019). Sea-ice algal phenology in a warmer
608 Arctic. *Science Advances*, 5(5). <https://doi.org/10.1126/sciadv.aav4830>
- 609 Tivy, A., Howell, S. E. L., Alt, B., McCourt, S., Chagnon, R., Crocker, G., et al. (2011).
610 Trends and variability in summer sea ice cover in the Canadian Arctic based on
611 the Canadian Ice Service Digital Archive, 1960-2008 and 1968-2008. *Journal of*
612 *Geophysical Research: Oceans*, 116(3). <https://doi.org/10.1029/2009JC005855>
- 613 Tschudi, M. A., Meier, W. N., Stewart, J. S., Fowler, C., & Maslanik, J. A. (2019a). *EASE-*
614 *Grid Sea Ice Age, Version 4*. Boulder, Colorado, USA.
615 <https://doi.org/https://doi.org/10.5067/UTAV7490FEPB>
- 616 Tschudi, M. A., Meier, W. N., Stewart, J. S., Fowler, C., & Maslanik, J. A. (2019b). *Polar*
617 *Pathfinder Daily 25 km EASE-Grid Sea Ice Motion Vectors, Version 4*. Boulder,
618 Colorado, USA. <https://doi.org/https://doi.org/10.5067/INAWUW07QH7B>
- 619 Woodgate, R. A., Weingartner, T., & Lindsay, R. (2010). The 2007 Bering Strait
620 oceanic heat flux and anomalous Arctic sea-ice retreat. *Geophysical Research*
621 *Letters*, 37(1), 1–5. <https://doi.org/10.1029/2009GL041621>

622 Zhang, J., & Rothrock, D. A. (2003). Modeling global sea ice with a thickness and
623 enthalpy distribution model in generalized curvilinear coordinates. *Monthly*
624 *Weather Review*, 131(5), 845–861. [https://doi.org/10.1175/1520-](https://doi.org/10.1175/1520-0493(2003)131<0845:MGSIWA>2.0.CO;2)
625 [0493\(2003\)131<0845:MGSIWA>2.0.CO;2](https://doi.org/10.1175/1520-0493(2003)131<0845:MGSIWA>2.0.CO;2)
626